Physics of Nickel Clusters. 2. Electronic Structure and Magnetic Properties

B. V. Reddy, S. K. Nayak, S. N. Khanna,* B. K. Rao, and P. Jena

Physics Department, Virginia Commonwealth University, Richmond, Virginia 23284-2000

Received: November 19, 1997

Using a combination of classical molecular dynamics simulation and first principles molecular orbital theory, we provide the first comprehensive study of the equilibrium geometries, energetics, electronic structure, vertical ionization potential, and magnetic properties of Ni clusters containing up to 21 atoms. The molecular dynamics simulation makes use of a tight binding many-body potential, while the calculations based on molecular orbital theory are carried out self-consistently using the numerical atomic bases and the density functional theory. The adequacy of the molecular dynamics results on the energetics and equilibrium geometries is tested by comparing the results with those obtained from the self-consistent molecular orbital theory for clusters of up to six atoms. For larger clusters, equilibrium geometries were obtained from molecular dynamics simulation, and their electronic structure and properties were calculated using molecular orbital theory without further geometry reoptimization. Frozen core and local spin density approximations were used in the molecular orbital calculations. In small clusters ($n \leq 6$), the calculations were repeated by including all electrons and the gradient correction to the exchange−correlation potential. The calculated vertical ionization potential and magnetic moments of Ni clusters are compared with recent experimental data.

I. Introduction

The most distinguishing feature that makes clusters different from any other form of matter is their finite size. Due to the large surface-to-volume ratio, clusters exhibit[1] unique geometries and electronic and magnetic properties. The study of the evolution of the structural, electronic, and magnetic properties of clusters has become an important topic, as it bridges our understanding among atoms, molecules and solids. In this context the study of the coupling between cluster geometry and electronic structure is particularly interesting, as clusters, unlike their bulk phases, can exhibit[2] isomers that are energetically nearly degenerate. While the existence of cluster isomers can be inferred directly from reactivity experiments,[3] their precise structural identification remains a formidable problem both from theoretical and experimental perspectives. Experimentally, determination of cluster geometries is difficult, as the clusters are too large for spectroscopic probes and too small for diffraction probes. Theoretically, the number of local minima as well as the number of geometrical parameters increase so rapidly with size that finding the global equilibrium structure of clusters of a few dozen atoms becomes an almost impossible task. While systematic studies of the evolution of atomic and electronic structure, based on first principles calculations, are available for simple metal clusters containing tens of atoms, very few studies exist for transition metal clusters containing more than six atoms.

The nature of bonding among atoms in transition metal clusters is intermediate between the free electron behavior in alkali metal clusters and the strong covalent character in carbon and silicon clusters. In addition, the large number of d electrons bunched into closely spaced energy levels makes many of these clusters magnetic. Interestingly, it is because of these complexities that transition metal clusters exhibit rich physics and chemistry. Recently, several experimental studies of the electronic structure,[4] vertical ionization potential,[5] reactivity,[6] and magnetic moments of Ni clusters[7,8] containing up to several hundred atoms have been reported. Most of the interesting size-specific properties, however, emerge in clusters containing less than 100 atoms. The electronic structure probed through photodetachment spectroscopy[4] suggests that the electronic structure of Ni_n clusters approaches the bulk limit for $n > 14$, while that probed through the measurements of the vertical ionization potentials[5] puts this limit beyond $n = 100$. Similar controversies also exist in the magnetic moment measurement. While the magnetic moment measured by one group[7] does not approach the bulk limit even for $n = 740$, another group[8] finds this limit to be reached for $n \sim 200$. None of these experiments provide much insight into the real topology of clusters. However, Parks et al.[6] have used the reactivity of Ni clusters with N_2 as a function of N_2 pressure and temperature to shed light on cluster geometry. From the plateau in the N_2 uptake data and a large number of assumptions concerning the mechanisms for N_2 chemisorption, they deduced the most likely geometries of the Ni clusters. Recently we have analyzed[9] in detail these assumptions and compared the predicted geometries to our calculated values. Although the agreement between our calculated structures and those predicted by Parks et al. was good in some cases, large discrepancies still remain. We have argued that a closer and independent examination of the assumptions made by Parks et al. in interpreting the N_2 uptake is needed. Recently, Apsel et al.[8] have measured the magnetic moments of Ni_n clusters for $5 \leq n \leq 740$. They argue that their data can shed light not only on the geometries of clusters but also on the nature of surface magnetism.

A number of first-principles calculations of the geometries and binding energies of small Ni clusters containing up to six atoms have been carried out. However, there are large discrepancies in the calculated ionization potentials[10−17] and magnetic moments.[13,16,18−25] These discrepancies arise due to the particular choice of geometries, interatomic spacing, atomic basis functions, approximations in the exchange−correlation potentials, and the treatment of the core electrons. A few studies

S1089-5639(98)00262-X CCC: $15.00
Published on Web 02/12/1998

of the equilibrium geometries,[26] binding energies, and magnetic moments of larger Ni_n clusters ($n \leq 55$) based on empirical tight binding molecular dynamics simulation[21] are available. To our knowledge, there are no systematic studies of the evolution of the electronic structure, ionization potential, and magnetic moment available based on first-principles theoretical technique for larger clusters ($n > 6$).

In this paper we present the results of such a study. We first repeat the calculations of equilibrium geometries, binding energies, ionization potentials, and magnetic moments of Ni_n ($n \leq 6$) clusters using self-consistent molecular orbital theory. We examine in detail the effect of freezing the core potential, the local spin density versus generalized gradient correction to the density functional theory, and the choice of Gaussian versus numerical atomic basis functions in the construction of the molecular orbitals. Since the calculation of equilibrium geometries from first principles for larger ($n > 6$) Ni clusters is a very difficult task, we have used classical molecular dynamics simulation[9] that employs a tight binding form[27] for the many-body interatomic potential. To determine if this potential can correctly predict the equilibrium geometries, we have compared these geometries with ab initio results for $n \leq 6$ that we have obtained using various levels of theory and computer codes. The agreement we have obtained allows us to believe that our molecular dynamics simulation can provide reliable geometries for larger clusters. Using the molecular dynamics simulation, we obtain the equilibrium geometries of Ni_n clusters for $6 < n \leq 21$. The electronic structure, ionization potentials, and magnetic moments based on these geometries were then calculated self-consistently within the framework of the molecular orbital theory and the density functional method.

In section II we briefly discuss our theoretical procedure. The results on the equilibrium geometries, electronic structure, vertical ionization potential, and magnetic properties are discussed in section III. A summary of our conclusions is provided in section IV.

II. Theoretical Procedure

Obtaining the equilibrium geometries of clusters is of central importance as many of the interesting properties of clusters are directly related to the special atomic arrangements within a cluster. Since there are no direct experimental methods to determine cluster structure, it can only be achieved at this stage from theoretical calculations. Properties such as Raman vibrational frequencies, photoelectron spectra, ionization potentials, and magnetic moments can then be computed from these geometries and compared with experimental data. A good agreement between experiment and theory then provides indirect evidence of the accuracy of the predicted structure. Although this process appears to be a reasonable route to obtaining information on cluster structure, the existence of isomers with different geometrical arrangements can complicate the issue. To make things worse, the number of likely isomers increases dramatically with cluster size. For transition metal clusters, the calculations are further complicated due to the quasi-localized nature of the d electrons. Due to the large density of states at the Fermi energy, the transition metal clusters are often magnetic. Thus, it is necessary to calculate the equilibrium geometries for various spin multiplicities. The existence of clusters with different magnetic solutions, unfortunately, gives rise to convergence problems. It is for these reasons that no systematic understanding of the evolution of the electronic structure and properties of Ni clusters containing up to a couple of dozen atoms from first principles is available to date. In the following we describe two complementary theoretical schemes to achieve this goal: The classical molecular dynamics based on a tight binding formulation of the interatomic potential is used to obtain equilibrium geometries. The molecular orbital theory is then used to calculate the electronic structure and magnetic properties using these geometries. We now outline the salient features of these two methods.

A. Molecular Dynamics Simulation. Molecular dynamics simulation is a powerful technique for studying the equilibrium geometries of clusters. The motion of atoms can be followed by using Newton's equation provided one has an accurate knowledge of the interatomic potential. In principle, any atomic displacement causes the electronic cloud to shift, which then forces the atoms to move. Thus, the electronic and atomic motions are coupled self-consistently. Car and Parinello[28] pioneered a new technique where the molecular dynamics takes into account atomic motion as well as quantum mechanics of the electrons, thus avoiding the need to know a priori the form of the interatomic potential. In addition, the quantum molecular dynamics method provides both the atomic and the electronic structures. Currently, the quantum molecular dynamics simulation is carried out by expanding the electron wave functions in terms of plane waves. While this has been successfully applied to simple metals and semiconductors, its application to transition metal clusters has been rather limited since the d electrons that characterize these metals are quasi-localized and can be represented only by a very large number of plane waves. Furthermore, it is problematic to use the Car−Parinello method to simulate systems where the energy levels shift at the Fermi energy, as is the case with the transition metal clusters.

We have, therefore, used the conventional classical molecular dynamics approach. The interatomic potential is taken from the work of Finnis and Sinclair[27] and Sutton and Chen.[29] The potential has the form

$$V = \epsilon \sum_i \left[\frac{1}{2} \sum_{j \neq i} \left(\frac{a}{r_{ij}} \right)^n - c \rho_i^{1/2} \right] \tag{1}$$

where

$$\rho_i = \sum_{j=i} \left(\frac{a}{r_{ij}} \right)^m \tag{2}$$

Here a is the lattice constant for bulk Ni and r_{ij} is the distance between atoms i and j. ϵ, c, m, and n are parameters that have been obtained by fitting computed properties such as cohesive energy, bulk modulus, and surface relaxation of bulk Ni. The use of semiempirical interatomic potentials in the molecular dynamics simulation of small clusters raises an obvious question regarding the reliability of the cluster geometries. We will show in section III that the potential in eq 1 can yield reliable geometries corresponding to the ground state not only of the clusters but also of their isomers.

We have used constant energy molecular dynamics[9] for determining the structure of Ni clusters. Both velocity Verlet and fifth-order Gear-predictor algorithms[30] were used to integrate Newton's equations of motions with a time step of 5×10^{-15} s. The total linear and angular momentum is kept zero, and the energy is conserved to within 0.01%. Both the algorithms give similar accuracy, and the results presented here are obtained using the velocity Verlet algorithm. Various random structures were generated and were assigned high velocities so that the clusters are in the liquid state, where they can visit many possible structures. Typically 100 different high-

energy initial structures are used for each cluster $n < 13$. A fewer number of structures (typically ∼50) are chosen for clusters $n > 13$. Starting from such structures, the minimum energy structure is obtained using either the steepest descent method or the simulated annealing method where the potential energy is taken as the control functional or by a combination of both methods. The structures thus obtained are cataloged and ordered by energy. Starting from the lowest energy structure, the cluster is heated slowly following the method suggested by Brian and Burton.[30] The clusters were equilibrated for 5×10^5 MD steps at each energy, and the ensembles are computed from the final portion of 3×10^5 MD trajectories. The temperature of the cluster is obtained from the average kinetic energy by the relation

$$T = \left[\frac{2}{3N-6}\right] E_{\text{kin}}/k_{\text{B}} \tag{3}$$

where k_{B} is the Boltzmann constant, $(3N - 6)$ represents the total number of internal degrees of freedom, and E_{kin} is the kinetic energy of the cluster.

B. Molecular Orbital Theory. Once the equilibrium geometries were obtained from molecular dynamics simulation, we calculated the electronic structure and properties of Ni clusters using the self-consistent-field−linear combination of atomic orbitals−molecular orbital (SCF−LCAO−MO) method.[31]

The exchange−correlation term in the potential is approximated by using the density functional theory.[32,33] Here, we have used two levels of approximations: the local spin density and the generalized gradient correction.[34] In the computation of the electrostatic potential, it is customary to freeze the inner cores of the atom, as these electrons seldom take part in the bonding and/or electronic structure and properties. We have, however, examined the validity of this approximation by repeating calculations including all electrons for Ni_n clusters with $n \leq 6$ and $n = 13$. We have also used two different basis sets to represent the atomic orbitals. In one, the wave function is described numerically on a radial mesh, while in the other, the basis functions are represented by a set of Gaussian orbitals. Errors can often be introduced by using an incomplete basis. We have examined the effect of basis sets by repeating the calculations using both the numerical and the Gaussian basis. For the former we have used ($3d^9 4s^1$) functions with a 4p polarization and the DMOL software,[35] while for the latter we have used (14s9p5d/9s5p3d) functions and the Gaussian 94 software.[36] The geometries for $n \leq 6$ are globally optimized by starting with an initial structure and optimizing the total energy without symmetry constraint. The forces at the atomic sites were computed by using the gradient technique, and the atoms were moved to new locations following the path of steepest descent. We have performed calculations for $n < 6$ using both these procedures to examine how sensitive our results are to different theoretical approach. To determine the ground state, we computed the total energies corresponding to the equilibrium structure for several spin multiplicities. This is needed since most clusters have several close lying multiplets. For each multiplicity, the equilibrium geometry, including possible Jahn−Teller distortion, is different. Therefore, one has to investigate all the multiplicities to find the true ground state. In the DMOL code, we used the aufbau principle with fractional occupation. We found that the ground state of clusters calculated using both the DMOL and Gaussian 94 codes have identical spin multiplicities. For larger clusters ($6 < n < 21$), we have used the geometries obtained in the molecular dynamics simulation. Without further reoptimization, we have then calculated the electronic structure (molecular energy levels), total energy, vertical ionization potential, and magnetic moments using the DMOL code. A detailed analysis of the geometry of Ni_{13} at the first-principles level of theory is also carried out by starting with the perfect icosahedric structure (as obtained from the molecular dynamics simulation) and allowing the structure to distort under reduced symmetry constraint. The ionization potential and magnetic moments of the distorted structures were calculated and compared with that of the perfect icosahedric structure to examine the extent to which these results are sensitive to Jahn−Teller distortions.

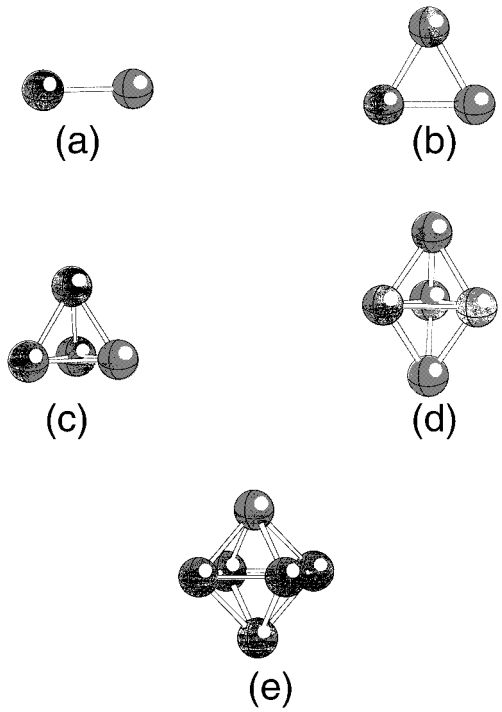

Figure 1. Equilibrium geometries of small ($n \leq 6$) Ni clusters.

III. Results

The central prerequisite in the computation of electronic structure and properties of clusters is their equilibrium geometries. Since for clusters $n > 6$ we are using the empirical interatomic potential and molecular dynamics simulation to obtain the geometries, it is important to ensure that the potential is accurate enough to describe the geometries and bond lengths of clusters not only for their ground states but also for their isomers. This is particularly important since the parameters in eq 1 are primarily obtained by fitting to bulk data. In addition, eq 1 does not contain any spin-dependent term, although magnetic effects are implicitly included by fitting to properties of ferromagnetic Ni. We first demonstrate the reliability of the potential in eq 1 to predict geometries, bond distances, and relative stabilities of small clusters ($n \leq 6$) by comparing the results with ab initio calculations.

A. Reliability of the Geometries Obtained from Classical Molecular Dynamics. In Figure 1 we give the equilibrium geometries of Ni_n ($n \leq 6$) clusters calculated from first principles using DMOL software and the LSDA level theory. The geometries agree with those calculated recently by Salahub and co-workers[24,47] using Gaussian basis sets and local spin density approximation. The molecular dynamics (MD) simulations using the potential in eq 1 also yield the same geometries for the ground state. The bond lengths calculated using the first-principles theory (DMOL) and the MD simulation are presented

TABLE 1: Bond Lengths and Binding Energies/Atom of Ni_n Clusters ($n \leq 6$) Calculated Using Different Levels of Theory

quantity	method	Ni_2	Ni_3	Ni_4	Ni_5	Ni_6	Ni_{13}
bond lengths (Å)	DMOL	2.06	2.17	2.24	2.29, 2.24	2.28	2.29
	MD	2.01	2.15	2.20	2.36	2.43	2.26
	ref 47	2.05	2.16	2.15, 2.28	2.36, 2.31		
	expt	2.155 ± 0.01					
binding energy (eV)	DMOL	3.15	3.74	4.08	4.43	4.67	5.36
	MD	2.10	2.50	2.77	2.90	3.03	3.39
	ref 47	1.82	2.40	2.82	3.07		
	expt	1.034					

TABLE 2: Geometries, Bond Lengths, and Binding Energies of Ni_4 and Ni_{13} Isomers Calculated Using MD and DMOL

		bond length (Å)		binding energy/atom (eV)	
cluster	geometry	DMOL	MD	DMOL	MD
Ni_4	tetrahedron	2.24	2.20	4.08	2.77
	square	2.15	2.12	3.93	2.61
Ni_{13}	icosahedric	2.29	2.26	5.36	3.39
	cuboctahedric	2.29	2.35	5.31	3.34

in Table 1 and compared with the local spin density results of Castro et al.[47] Note that for Ni_2 and Ni_3 the bond lengths computed using the MD method agree very well with the first-principles calculations. For Ni_4, both DMOL and MD methods yield a perfect tetrahedron as the ground state, while the calculations in ref 24 yield a slightly Jahn−Teller distorted structure. Again the MD bond lengths agree with first-principles calculations to within 0.1 Å. Similar is the case for Ni_5. We will show in the following that the ionization potential and magnetic moment computed for the distorted geometry are insensitive to the mild distortion in the geometry.

The binding energies calculated using the MD approach are also compared with first-principles calculations in Table 1. Although the binding energies computed for each of these clusters differ from those computed from first principles, the relative variation with cluster size is consistently predicted by the MD calculation. We should also note that the binding energies are almost always overestimated in the LSDA level of theory, and for Ni_2, where experimental result exists, the binding energy calculated from MD is closer to experiment than the first-principles DMOL result. We should remind the reader that in the present paper the only use of MD calculation is to provide the geometry. The electronic structure is handled by first-principles theory.

Since the potential in eq 1 has no explicit spin-dependent term, we have examined the influence such a term can have on equilibrium geometry and bond lengths. We have done this by optimizing the geometry of Ni_5 within the local density approximation (LDA) and comparing the results with those given by using LSDA in Table 1. The corresponding bond lengths are 2.28 and 2.24 Å and agree with the LSDA results within 0.01 Å. We should also point out that Andriotis et al.[21] have recently examined this issue by incorporating the Hubbard approximation, which contains magnetic exchange, into the tight binding molecular dynamics. They have found that the inclusion of the on-site correlations does not change the geometries of the Ni_n clusters, although magnetic effects strongly influence the structure of Fe_n clusters. Thus we can conclude that the geometries and bond lengths of Ni clusters would be hardly influenced by having an explicit spin-dependent term in the potential.

Since a cluster can have many isomers, it is important that the MD calculations can also yield the relative stability of various isomers reliably. To illustrate this capability, we have studied the next higher energy isomer of Ni_4 and Ni_{13}. In Figure 2 we plot the geometries of these isomers of Ni_4 and Ni_{13}, which

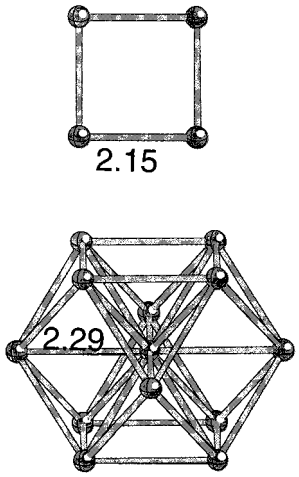

Figure 2. Geometries of isomers of Ni_4 and Ni_{13} clusters. These correspond to energies just above the ground states.

are square and cuboctahedral, respectively. Both MD and first-principles DMOL calculations yield the same geometries of the isomers. The corresponding bond lengths and binding energies of these isomers are given in Table 2. Note that MD simulation using the potential in eq 1 indeed is able to give the correct ordering of isomers (see Tables 1 and 2). Thus, we are confident that the potential in eq 1 is able to yield reliable ground-state geometries of Ni clusters.

B. Equilibrium Geometries and Binding Energies of Ni_n ($n \leq 21$) Clusters. Using the potential in eq 1, we have recently calculated the geometries for Ni_n clusters containing up to 23 atoms. The results have been published recently.[9] For the clarity of the discussion to follow, we outline only briefly the salient features of these geometries and refer the reader to our earlier paper[9] for details. The geometries of Ni_n clusters ($n \leq 6$) resemble closely those found in rare-gas systems; namely, they are symmetric and close-packed. The structures of Ni_3, Ni_4, Ni_5, and Ni_6 are respectively equilateral triangle, regular tetrahedron, triangular bipyramid, and distorted octahedron with a D_{4h} symmetry. Ni_7 exhibits two isomers, a capped octahedron and a pentagonal bipyramid, which are energetically nearly degenerate. The larger clusters evolve with a 5-fold ring as a common backbone leading to Ni_{13}, which becomes a nearly perfect icosahedron. For Ni_{14} and larger clusters, the added atoms, instead of capping the faces of the Ni_{13} cluster, do form 6-fold rings. However, Ni_{19} once again shows icosahedric growth. As cluster size increases further, it becomes increasingly difficult to visualize the growth pattern. It is more

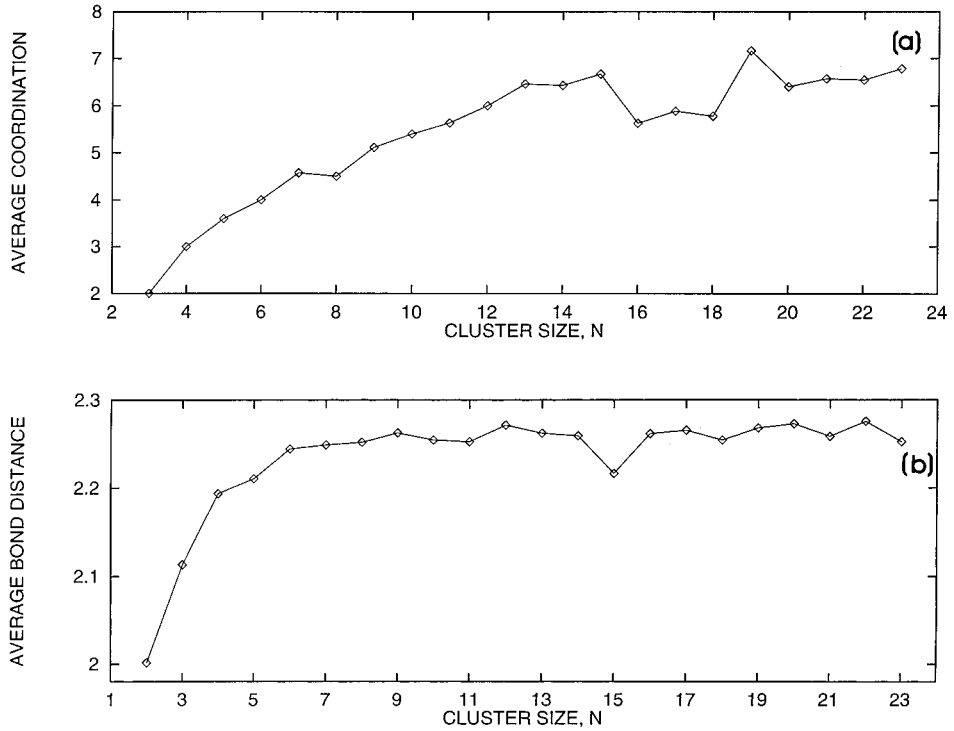

Figure 3. The evolution of (a) the average coordination number and (b) the interatomic distance of Ni clusters as a function of size.

meaningful then to examine the evolution of the coordination number that characterizes the number of nearest neighbors an atom has in a cluster. Note that in bulk Ni, which has a fcc structure, this number is 12, and for an atom on the (111) surface, the coordination number is 9.

The average coordination number in a cluster is defined as

$$\mathrm{CN} = \frac{1}{N}\sum_i N_i \tag{4}$$

where the ith atom has N_i number of nearest neighbors. N is the total number of atoms in the cluster. In Figure 3a we plot the average coordination number as a function of cluster size. Note that the coordination number rises steadily until $n = 15$ and then exhibits some minor oscillations. Even for the largest cluster studied, i.e., $n = 23$, the coordination number is far from the bulk value of 12. This is what is expected since for all these clusters most atoms are surface atoms and the coordination number for crystalline surface is less than 9. In Figure 3b we plot the size dependence of the average bond distance in these clusters. Note that the interatomic distances rise steadily and show some oscillatory behavior beyond $n = 14$. The oscillations in the coordination number and interatomic distance are not common in simple metal clusters and result due to unique bonding characteristics in transition metal systems. We will show in the following that the evolution of the coordination number and interatomic separation has a strong effect on the electronic structure and magnetic moments of Ni clusters.

Using the geometries derived from the molecular dynamics simulation, we have calculated the total energies based on the self-consistent molecular orbital theory and the local spin density approximation. The binding energy/atom is calculated using the equation,

$$E_b(n) = -[E(n) - nE_0]/n \tag{5}$$

where $E(n)$ is the total energy of the n-atom cluster and E_0 is the energy of the free atom. We have plotted these energies in Figure 4 and compared them to the corresponding values obtained previously from the molecular dynamics simulation. Note that while there are significant quantitative differences between the binding energies calculated by these two methods, their systematics remain unaffected; namely, both calculations yield a fairly monotonic increase in the binding energies with no anomalous feature that can point to the existence of magic numbers, as has been found in alkali metal clusters.

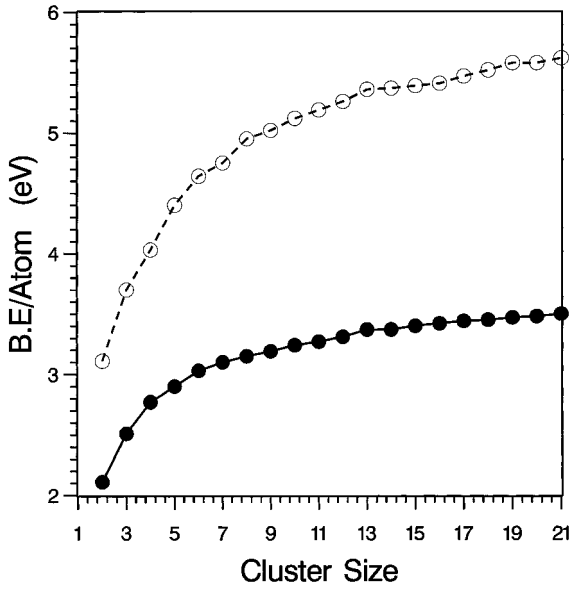

Figure 4. Comparison between the binding energies of Ni_n clusters calculated from molecular dynamics simulation (solid circles) and self-consistent molecular orbital theory (open circles).

C. Electronic Structure and Vertical Ionization Potential. The understanding of the evolution of the electronic structure as atoms coalesce to form clusters of increasing size is just as important as the understanding of the evolution of their atomic structure and binding energies. As pointed out earlier, neither the geometries nor the coordination numbers of Ni_n clusters for

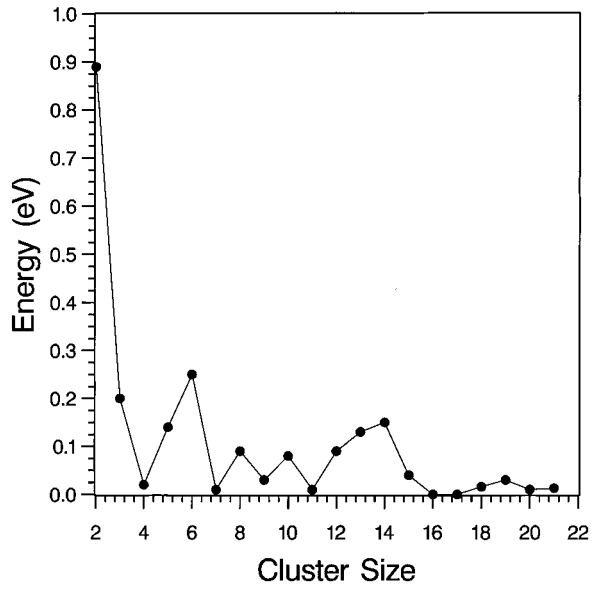

Figure 5. Energy gap between highest occupied molecular orbital (HOMO) and lowest unoccupied molecular orbital (LUMO) of Ni_n clusters.

$n \leq 23$ resemble the bulk. Does this mean that the electronic structures of these Ni clusters are also far from being bulklike? Fortunately, experiments can probe the evolution of the electronic structure of clusters far better than they can probe the geometries. One of these techniques is based on the photoelectron spectroscopy. Here a size-selected cluster anion is photodetached by a fixed-wavelength photon. The photoemitted electrons, which carry the electronic structure information of the neutral clusters, are then energy analyzed. A systematic study of the photoelectron spectra can then illustrate how the electronic structures of clusters change from discrete levels to bandlike as cluster size increases. Wang and Wu[4] have measured the photoelectron spectra of Ni_n clusters for $1 < n < 50$. They have observed an odd−even alternation in the electron affinities for $1 < n < 5$, with even clusters having lower electron affinities and sharper features near the threshold compared to the odd clusters. The spectra beyond Ni_{14} show little change as cluster size increases. This would seem to imply that the bandlike states of Ni clusters have already emerged in clusters as small as $n = 14$. Note that the interatomic distance and binding energies shown in Figures 3 and 4 do not vary strongly for $n > 14$, but are far from the bulk limit.

We have computed the molecular orbital energy values for both spin-up and -down states self-consistently for clusters containing up to 21 atoms by using the equilibrium geometries discussed earlier. In Figure 5 we show the energy gap between the highest occupied molecular orbital (HOMO) and lowest unoccupied molecular orbital (LUMO). Note that beyond $n = 14$ the HOMO−LUMO gap essentially ceases to exist and the energy levels come so close to each other that they appear bandlike. Since the photoelectron detachment spectroscopy primarily measures the density of states of the neutral clusters, it is easy to see that the size specificity loses its significance beyond $n = 14$. This is in agreement with the work of Wang and Wu.[4]

The electronic structure information can also be extracted from the near-threshold photoionization efficiency (PIE) experiments. Here one measures the ionization potential of the neutral clusters. The PIE spectra are broadened if the geometry of the cluster undergoes significant modifications during the photoionization process. This effect is particularly pronounced for small clusters, as their geometries are most likely to change upon ionization. In very large clusters approaching the bulk limit, removal of a single electron is not expected to cause structural modification. Knickelbein et al.[37] have measured the vertical ionization potential (defined as the energy needed to remove an electron from a neutral cluster without modifying its geometry) of Ni_n clusters for $3 < n < 90$. We begin with a qualitative discussion of their results. (1) The ionization potentials do not exhibit any sharp drops for particular cluster sizes, as has been the hallmark in all alkali metal clusters. These along with the lack of clear maxima in the binding energies in Figure 4 indicate that there are no magic clusters in Ni. (2) The ionization potential exhibits strong size dependence for $n \leq 11$ and approaches relatively smoothly and nearly monotonically from 5.84 eV for Ni_{11} to 5.56 eV for Ni_{90}. Note that (100), (110), and (111) surfaces of bulk Ni have work functions (WFs) of 5.22, 5.04, and 5.35 eV, respectively. Thus, from the PIE experiment, the electronic structure of Ni_{90} could be thought of as being different from the bulk value since the ionization potential does not lie in the range 5.04−5.35 found in the bulk. This is in sharp contrast to the conclusion of Wang and Wu[4] that the electronic structure of Ni_{14} is already bulklike.

A large number of theoretical calculations[10−17] of the electronic structure and vertical ionization potential of small ($n \leq 6$) Ni clusters is available in the literature. However, most of these calculations either have used the bulk geometry and bulk interatomic distance for the Ni clusters or are based on semiempirical methods. Only a few calculations are available where the geometries of small Ni clusters have been globally optimized. In Table 3 we provide a summary of the previous theoretical results on the vertical ionization potential. As can be seen, the results vary over a wide margin. It is difficult to pinpoint whether the discrepancy between theory and experiment is due to poor choice of geometry, interatomic distance, and/or the calculational method.

In this paper, we provide the first systematic study of the vertical ionization potential of Ni_n clusters containing up to $n = 21$ atoms. Our results are obtained from total energy calculations of the neutral and singly ionized clusters using the self-consistent molecular orbital theory. The vertical ionization potential is given by

$$\mathrm{IP} = E(\mathrm{Ni}_n^{+}) - E(\mathrm{Ni}_n) \tag{6}$$

where $E(Ni_n)$ is the total energy of the neutral cluster and $E(Ni_n^+)$ is the total energy of the corresponding singly charged cluster having the neutral geometry. The results are compared with the experimental data in Figure 6. Note that calculated ionization potentials reproduce the systematics rather well; namely, they are very sensitive to cluster size in the range $2 \leq n \leq 7$. Beyond this range, the maximum difference in the calculated IPs between any two clusters is about 0.4 eV. Experimentally, this number is 0.3 eV. What is noteworthy is that the experimental IPs show little fluctuation with size beyond $n = 11$, while theoretically the IPs of clusters with $n = 13$ and 18 show clear maxima.

The quantitative agreement between theory and experiment is, however, not perfect, although most calculated values agree with experiment to better than 10%. Now let us discuss the possible sources for this discrepancy. (1) One obvious reason could be that the geometry obtained from the molecular dynamics may not be as accurate as one would expect from an ab initio theory (assuming it could be obtained!). Interestingly, the maximum disagreement between the calculated and experimental IP is not for large ($n > 7$) clusters, but rather for smaller

TABLE 3: Summary of Calculated Vertical Ionization Potentials (eV) for Small Ni_n ($n \leq 6$) Clusters

authors	method	Ni_2	Ni_3	Ni_4	Ni_5	Ni_6
Blyholder[a]	ref 10	6.8	6.5	6.3	6.3	6.3
Adachi et al.[b]	ref 11					5.1
Basch et al.[c]	ref 12	5.4	3.9	4.4	4.7	4.9
Rösch et al.[d]	ref 13					5.85
Nygren et al.[e]	ref 14			6.08	5.83	6.65
Wolf & Schmidtke[f]	ref 15	3.4				
Tomonari et al.[g]	ref 16	5.7	4.2	5.1	4.8	4.4
Pastor et al.[h]	ref 17	6.5	6.2	6.2	5.9	5.6
present work[i]		8.3	6.8	5.9	6.6	6.8
experimental	refs 52, 53	7.6	6.12	5.70	6.20	6.78

[a] CNDO. [b] DVM-X α with symmetry constraint optimization. [c] ECP SCF−CI [bulk fragments with a fixed bulk nearest neighbor distance] [d] LCGTO-LSD [fixed bulk Ni−Ni distance]. [e] ACPF+CPP [fixed bulk nearest neighbor distance]. [f] SCF-LCAO-MO-RHF. [g] SCF-LCAO-MO/CI [bulk Ni−Ni distance is fixed for N = 4, 5, and 6]. [h] Tight binding method [nonoptimized geometries]. [i] SCF-LCAO-MO/DFT.

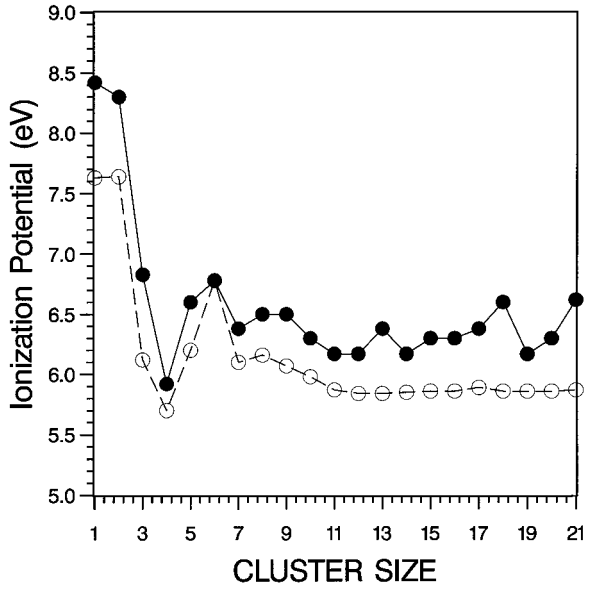

Figure 6. Comparison between theoretical (solid circles) and experimental (open circles) ionization potentials of Ni clusters.

TABLE 4: Comparison of Calculated Vertical Ionization Potentials and Magnetic Moments/Atom of Ni_4, Ni_5, and Ni_{13} Using Geometries from MD and DMOL Procedures

quantity	method	Ni_4	Ni_5	Ni_{13}
vertical ionization potential (eV)	DMOL	5.92	6.60	6.32
	MD	5.81	6.46	6.38
magnetic moment/atom (μ_B)	DMOL	1.0	0.8	0.62
	MD	1.0	0.8	0.62

clusters ($n \leq 6$), where geometries are obtained from first principles. For example, our calculated IP for Ni_3 is 0.7 eV larger than the experimental value. To examine what errors minor changes in the geometries can cause, we have calculated the vertical ionization potentials and magnetic moments of Ni_4, Ni_5, and Ni_{13} using the geometries (with corresponding bond distances) obtained from both the MD simulation and the first-principles (DMOL) theory. The results are compared in Table 4. Note that the vertical ionization potentials change by about 0.1 eV, while the magnetic moments remain unaffected when one uses MD-based geometries. (2) The second source of error could be our use of the frozen-core and local spin density approximation. We have, therefore, repeated our calculations of the equilibrium geometries, binding energies, and ionization potentials using molecular orbital theory with all electrons and generalized gradient approximation. All levels of theory give identical geometries, which are given in Figure 1. The corresponding structural parameters, binding energies, and IPs are given in Table 5. Note that the bond distances, binding energies, and ionization potentials are essentially unaltered whether one uses all electron or frozen-core approximation at the same level of exchange−correlation potential. However, the energetics (binding energies and vertical ionization potentials) are different when the generalized gradient approximation is used for the exchange−correlation potential. The binding energies are lowered as are the vertical ionization potential, bringing theory to closer agreement with experiment with the exception of Ni_6. (3) We next discuss the possible effect temperature may have on the ionization potential. It is expected that open shell systems such as transition metal clusters of Ni should be characterized by a number of low lying excited states. This is supported by theoretical calculations that predict a high density of states at the Fermi energy that increases with cluster size and symmetry. The photoelectron spectra of Ni_3 through Ni_{18} recorded by Gantefor et al.[38] also indicate a very high density of electronic states lying just above the highest occupied molecular orbital (HOMO). The electronic states within 0.1 eV are comparable to the thermal energies of the clusters and hence are accessible by the clusters produced by laser vaporization in the absence of effective cooling techniques. One then wonders if the electrons in these allowed transitional states affect the IPs of the clusters.

The study of temperature dependence of structure and properties of clusters should be ideally carried out by taking into account the coupling between electronic and atomic motion self-consistently. While the Car−Parinello method[28] can, in principle, accomplish this goal at any temperature, its application to transition metal systems is difficult as mentioned before. Therefore, an alternate route has to be found to at least qualitatively assess the effect of temperature. We are working toward such a goal, and the results will be published in due course.

In summary, a quantitative understanding of the experimental ionization potential would require a theory that goes beyond the local spin density approximation and includes the effect of temperature. We note that the effect of the gradient correction in the exchange−correlation potential is to lower the ionization potential. Interestingly, the theoretical values based on 0 K structure and local spin density approximation are larger than experiment (see Figure 6). The gradient correction alone, unfortunately, does not bring theory into quantitative agreement with experiment. A realistic treatment of the effects of temperature may be needed for this purpose.

D. Magnetic Moments. The study of the magnetic properties of low-dimensional systems such as surfaces, multilayers, and nanoparticles in the past few years has clearly demonstrated not only that the magnetic moments of ferromagnetic elements are enhanced over the bulk value[39] but nonmagnetic elements could also exhibit magnetic order.[40] These observations have

TABLE 5: Comparison of Our Results from Various Levels of Theory

	bond length (Å)			binding energy/atom (eV)			ionization potential (eV)			
cluster size, *n*	all-electron LSD	frozen-core LSD	frozen-core GGA	all-electron LSD	frozen-core LSD	frozen-core GGA	all-electron LSD	frozen-core LSD	frozen-core GGA	expt
2	2.06	2.06	2.09	3.15	3.11	2.64	8.34	8.30	7.89	7.6
3	2.17	2.17	2.24	3.74	3.70	3.00	6.86	6.83	6.38	6.12
4	2.24	2.24	2.30	4.08	4.04	3.17	5.90	5.92	5.43	5.70
5	2.29	2.29	2.35	4.43	4.40	3.44	6.58	6.60	6.01	6.20
	2.24	2.24	2.31							
6	2.28	2.27	2.33	4.67	4.64	3.58	6.78	6.82	6.34	6.78
	2.28	2.29	2.33							

generated a lot of interest in the study of magnetism of clusters. As already discussed, most atoms in clusters are surface atoms, and clusters can, therefore, be classified as low-dimensional systems. Clusters of magnetic elements are expected to possess enhanced magnetic moments,[41] while clusters of nonmagnetic elements could sustain magnetic order.[42] It is also expected that clusters can be used to study the evolution of surface magnetism since in the limit of infinite size the surface of a cluster should resemble that of a crystal.[7]

Clusters, however, possess other unique features that are not common to crystal surfaces and multilayers. Among these are their unique structures, atomic coordinations, and interatomic distances. Theoretical studies[43] have indicated that the magnetic moment is an indicator of the overlap of electron distribution between neighboring sites: the greater the overlap, the lower the moment. Thus, an increase in atomic coordination would tend to reduce the moment, while an increase in the interatomic distance would enhance the moment. In addition, the cluster symmetry also plays a role. For example, a 13-atom cluster exhibiting icosahedric shape would have a different magnetic moment than if it is cuboctahedric. Since the geometry, atomic coordination, interatomic distance, and symmetry depend strongly on size, the study of magnetism of clusters can provide unique insight into the fundamental origin of magnetism.

Early experiments[44] on size-selected Fe clusters consisting of up to several hundred atoms produced some interesting results. (1) The effective magnetic moment, μ_{eff}, per atom of a cluster was smaller than the bulk magnetic moment and increased with cluster size. This is contrary to what one would have expected from a wealth of data on magnetism of low-dimensional systems such as surfaces and multilayers. Due to low coordination number in clusters (see Figure 3),[43] the magnetic moment per atom of a cluster should be larger than the bulk value and should decrease with increasing size. (2) The effective magnetic moment of a cluster increases with increasing magnetic field. In the bulk the magnetic moment/atom is independent of the field. (3) The last, and perhaps the most important, aspect of cluster magnetism is associated with its temperature dependence. While one experimental group observes that the effective magnetic moment *increases* with temperature, another experimental group reports just the opposite.[45] Note that in bulk ferromagnetic metals, the magnetic moment of the atom is independent of temperature, while the average magnetization decreases with temperature. These unique observations have led one to wonder if cluster magnetism is fundamentally different from bulk magnetism.

The size and field dependence of cluster magnetism has been successfully explained by the superparamagnetic model, where the cluster is considered to be a ferromagnetically aligned single domain.[46] The anisotropy energy is assumed to be much smaller than the thermal energy. During the residence time of the cluster in the magnetic field, the intrinsic magnetic moment, under thermal agitation, explores much of the Boltzmann distribution of magnetic moment orientations in space. This leads to the Langevin function for the time-averaged magnetic moment per atom, μ_{eff}:

$$\mu_{\text{eff}} = \mu\left[\coth\left(\frac{N\mu B}{k_{\text{B}}T}\right) - \frac{k_{\text{B}}T}{N\mu B}\right] \tag{7}$$

where μ is the intrinsic magnetic moment per atom, N is the number of atoms in the cluster, B is the applied magnetic field, T is the temperature, and k_{B} is the Boltzmann constant. For a fixed temperature, T, the above formula explains the observed field and size dependence of the average magnetic moment.

The computation of the intrinsic moment, μ, from eq 7 can be simplified in the limit $N\mu B \ll k_{\text{B}}T$. With this assumption, eq 7 leads to

$$\mu_{\text{eff}} = (N\mu)^2 B/3k_{\text{B}}T \tag{8}$$

Since in a Stern−Gerlach experiment B and N are known, μ can be easily calculated from the measured value of μ_{eff} only if the cluster temperature T is known precisely. There is considerable controversy in the literature concerning how accurately the cluster temperature can be determined. While for very small clusters, the temperature has been unambiguously determined, it is believed that the task is very difficult for large clusters. In addition, even if the cluster temperature is precisely known, eq 7 will yield only the magnetic moment, μ, at that temperature. Since theoretical calculations are done at 0 K, a quantitative comparison between theory and experiment can be done only if μ can be computed at the cluster temperature. As we have already seen in the previous section, the temperature can have significant impact if for a given cluster the spacings between energy levels near the HOMO level is comparable to $k_{\text{B}}T$.

Recently Apsel et al.[8] have measured the effective moment of Ni_n clusters containing 5−740 atoms using a Stern−Gerlach magnet. They have then used eq 7 to extract the intrinsic moment per atom, μ, by taking the cluster temperature to be 73−198 K. There are several interesting features to note. (1) The intrinsic moments, as expected, are indeed larger than the bulk value of $0.6\mu_{\text{B}}$ and do not even approach the bulk limit for $n = 740$. (2) The magnetic moment of Ni_5 is almost 3 times the bulk value and decreases rapidly to a value of $0.9\mu_{\text{B}}$ for Ni_{13}. (3) The variation in the moment is nonmonotonic and shows distinct minima at $n = 13$, 34, and 58.

We first provide a qualitative discussion of their results. The enhancement of magnetic moments in clusters over the bulk value is due to low coordination (see Figure 3). Apsel et al. have argued that their results can illustrate the magnetic properties of surfaces. Note that the cluster surfaces are entirely different from crystal surfaces. For example, the magnetic moment of surface atoms in Ni(100)[39] is $0.68\mu_{\text{B}}$, which is only marginally enhanced over the bulk value of $0.6\mu_{\text{B}}$. On the contrary, the magnetic moment of the largest cluster Bloomfield

et al. have measured is about $0.9\mu_B$. More importantly, the magnetic moment drops by a factor of 2 from Ni_5 to Ni_{12}. In this range, all atoms are surface atoms. Thus, it is very difficult to relate cluster magnetism to crystal surface magnetism. What is important in cluster magnetism is not that most atoms are surface atoms, but that their coordination number varies strongly with size. This variation is linked to the topology of the clusters. This can be seen by comparing the results in Figure 3 with the experiment.[8] We note that the coordination number steadily rises with cluster size and is far from the crystal surface value of 9. Since the magnetic moment decreases with increasing coordination, the experimental results can be qualitatively understood. We will show in the following that a quantitative understanding requires far more than just counting the number of surface atoms versus bulk atoms.

A number of calculations of magnetic moments with varying degrees of approximations have been carried out for small Ni clusters.[13,16,18−25] The calculated values vary over wide ranges. For example, for Ni_3, the calculated values[13,16,18,21,25] for the moment per atom range from $0.67\mu_B$/atom to $1.33\ \mu_B$/atom. For Ni_4, the values range from 0.5 to $1.5\mu_B$/atom[16,19,21,22,24,25], for Ni_5, from 0.8 to $1.6\mu_B$/atom,[13,16,21,24,25] and for Ni_6 from 1 to $2.0\ \mu_B$/atom.[13,16,19,20,21,25] Part of the discrepancy arises because some authors have assumed the geometry of the Ni clusters to be bulklike with bulk interatomic spacing. Since the magnetic moments are sensitive to cluster geometry and interatomic separation, a comparison of these results with the experimental value or with ab initio calculations that make use of optimized geometries is not very fruitful. What is discomforting is that magnetic moments calculated using optimized geometries by various authors are not in agreement. Note that for Ni_3, our computed moments of $0.67\mu_B$/atom agree with the calculations of Khanna and Reuse,[25] who used pseudopotentials, local spin density approximation, and Gaussian orbitals, but disagree with those obtained using the configuration interaction technique. However, for Ni_4, our calculated moment disagrees with that derived by Khanna and Reuse. Unfortunately, there are no experiments on Ni_3 and Ni_4 that can be compared with theory. For Ni_5, however, an experimental result does exist. The experimental moment/atom is $1.8\mu_B$. This is close to the value of $1.6\mu_B$ calculated by Khanna and Reuse, which is a factor of 2 larger than that presented here. We would like to add that Castro et al.[47] have recently calculated the moments of Fe_n, Co_n, and Ni_n clusters containing up to five atoms using Gaussian basis and density functional theory. They obtain a moment of $0.8\ \mu_B$ for Ni_4 and $1.0\ \mu_B$/atom for Ni_5, which agrees with our present results. The calculations carried out by Khanna and Reuse[25] employ norm-conserving pseudopotentials which are based on atomic calculations including relativistic effects and vacuum polarization. The pseudopotentials, however, do not take into account the polarization of the atomic cores. These authors have now carried out a nonrelativistic all-electron calculation similar to those reported here and find the same results for the magnetic moments as reported in Table 6. It will be interesting to see if relativistic effects are important by carrying out an all-electron calculation, including the relativistic effects.

To gain further confidence in our present results, we have repeated the calculations up to $n = 5$ using Gaussian basis and Gaussian 94 software. We have also used two levels of approximation in the exchange−correlation potential (local spin density vs generalized gradient). In addition, we have carried out all-electron calculations and compare these with the results of the frozen-core calculation. The geometries are optimized at each of these levels. The results calculated using both DMOL and Gaussian 94 software for Ni_n ($n \leq 5$) are in agreement with each other and are given in Table 6. We also note that the freezing of the core and/or using local spin density approximation yields the same moments as when these approximations are avoided. The fact that our extensive analysis of Ni_5 results in a magnetic moment that also agrees with the recent calculation of Castro et al.[47] but differs markedly from experiment raises some serious concerns. We will discuss this more critically later in the section.

TABLE 6: Comparison between Magnetic Moments Calculated Using DMOL and Gaussian 94 Software for Ni_n ($n \leq 5$) Clusters Using Various Levels of Theory

	DMOL			
cluster size	all-electron LSD	frozen-core LSD	frozen-core GGA	Gaussian 94 effective core potential and GGA
2	1.00	1.00	1.00	1.00
3	0.67	0.67	0.67	0.67
4	1.00	1.00	1.00	1.00
5	0.80	0.80	0.80	0.80

[a] For example, using a Gaussian 94 code, we found that for Ni_4 confined to a rhombus structure, multiplicities 3, 7, and 9 are 0.25, 0.21, and 2.6 eV above the ground state with a multiplicity of 5.

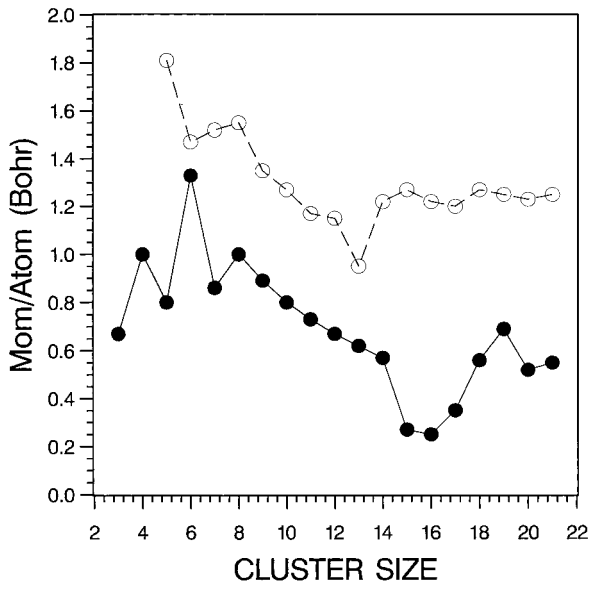

Figure 7. Comparison between calculated (solid circles) and experimental (open circles) magnetic moments of Ni_n clusters ($2 \leq n \leq 21$).

For clusters with $n > 6$ we have used the globally optimized geometries from our molecular dynamics simulation and the molecular orbital theory within the local spin density approximation to calculate the moments. This is in contrast to the calculation of Menon et al.,[21] who used the semiempirical tight binding theory to calculate the geometry as well as the moments. We believe that our study goes a step beyond what has been presented by Menon et al.

In Figure 7 we compare our calculated moments with the experimental result of Apsel et al. Note that the theory reproduces the general trend of the size dependence of the magnetic moment; namely, the magnetic moments are enhanced over the bulk value, vary nonmonotonically with size, and decrease significantly as cluster size increases from $n = 2$ to $n = 13$. In addition, the magnetic moment shows marked fluctuations at small sizes. To understand the origin of these changes, we carried out a Mulliken population analysis of the resulting charge density and the contributions of the s, p, and d electrons to the moment. While the d moment was around $0.8\mu_B$

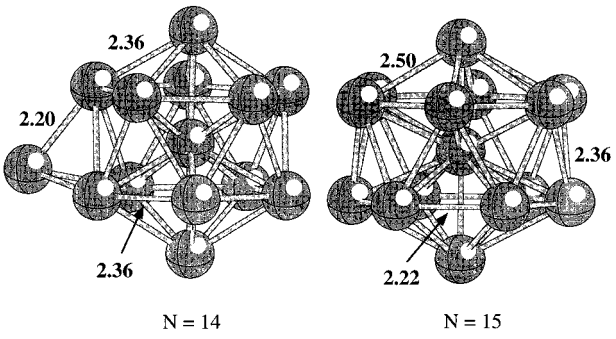

Figure 8. Equilibrium geometries of Ni_{14} and Ni_{15} clusters.

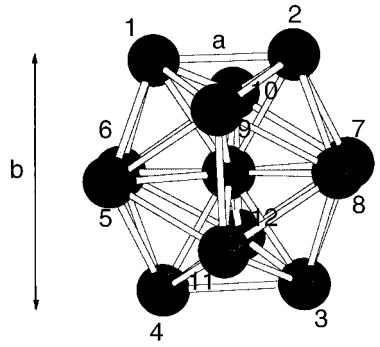

Figure 9. Icosahedric geometry of the Ni_{13} cluster.

in most cases, the combined s and p moment was −0.01, −0.08, 0.24, 0.08, 0.33, and 0.08 for Ni_2, Ni_3, Ni_4, Ni_5, Ni_6, and Ni_7, respectively. The fluctuations are, therefore, due to the variation in s and p polarization. We also found that these polarizations become negligible for clusters containing more than 14 atoms. The overall variation in the moment is consistent with the rapid rise in the coordination number shown in Figure 3. However, there are some serious quantitative differences between theory and experiment. For example, as mentioned before, the experimental value of the moment in Ni_5 is almost a factor of 2 larger than our calculated value. While experiment shows a small increase in the moment in going from Ni_6 to Ni_7, the theoretical value shows an abrupt decrease. The experimental moment shows a minimum at Ni_{13}, while the theory predicts a continuing decrease in the moment until $n = 16$.

We first examine these discrepancies individually. The sharp drop in the experimental moment on going from $n = 5$ to $n = 6$ was thought by Apsel et al. to be due to a geometrical effect, as Ni_5 is a triangular bipyramid and Ni_6 is a compact octahedron. Note that while the average coordination rises on going from Ni_5 to Ni_6 (see Figure 3), which should cause a decrease in the moment as observed, the average interatomic distance also increases from Ni_5 to Ni_6. This would tend to increase the moment of Ni_6 compared to Ni_5. Thus, these two factors act in opposite directions, and the quantitative nature of cluster magnetic moment cannot always be attributed to atomic coordination alone. On going from Ni_{13} to Ni_{14}, neither the average coordination nor the interatomic distance changes significantly (see Figure 3). Thus, it is surprising that the experimental magnetic moment of Ni_{14} is larger than that of Ni_{13}. We also predict Ni_{15} to be less magnetic than Ni_{14} in contradiction with the experiment. While the average coordination increases marginally on going from Ni_{14} to Ni_{15}, the average interatomic distance drops precipitously. Both these factors act in unison to decrease the moment of Ni_{15} compared to Ni_{14}, exactly as our calculated result shows in Figure 7. To demonstrate this more clearly, we show in Figure 8 the geometries of Ni_{14} and Ni_{15}. Note that the geometry of Ni_{14} evolves by capping one of the triangular faces of Ni_{13}, which is icosahedric and thus has an open structure. The structure of Ni_{15} is quite different: three coaxial atoms are connected to two hexagonal rings and Ni_{15} is much more compact than Ni_{14}. It is important to emphasize that the calculated geometries of Ni_{12}, Ni_{13}, and Ni_{14} are in agreement with the N_2 adsorption data of Riley and co-workers.[6]

To analyze where the blame for the above discrepancy lies, we first discuss the limitations in the theory that could contribute to this discrepancy. (1) First of all, the geometries we have used for $n > 6$ are those obtained from molecular dynamics simulation. Since the many-body potential did not contain an explicit magnetic term, it is legitimate to ask if these geometries could be in error and thus cause an error in the calculated magnetic moment. As noted before, the absence of a magnetic component in the potential has been shown to have little effect on the structure. Second, geometries calculated from molecular dynamics simulation agree perfectly with those obtained from ab initio spin-dependent calculations. More importantly, the worst disagreement between theory and experiment in Figure 7 is for Ni_5, for which the geometry was obtained from first principles. Since our computed magnetic moment of Ni_{13} also disagrees with the experimental trend, we have examined the geometry of this cluster in detail by using the ab initio theory. We allowed the cluster to undergo distortion by lowering the symmetry from I_h to D_{2h}. In Figure 9 we show the structure of Ni_{13} icosahedron, which could also be thought of as a central atom surrounded by three rectangles (atoms 1 2 3 4, 5 6 7 8, and 9 10 11 12) with sides a and b. With D_{2h} symmetry we varied a and b to minimize the energy at the local spin density molecular orbital level of theory. These values changed slightly from the perfect icosahedric shape. For a perfect icosahedron of Ni_{13}, $a = 1.9517$ Å and $b = 1.2061$ Å. In the present case, for the optimized structure with the D_{2h} symmetry, $a = 1.9687$ Å and $b = 1.1781$ Å. However, the magnetic moment remained at the initial value of $0.62\mu_B$. Note that several other authors have reported the same value for Ni_{13}.[25,48] (2) The results in Figure 7 are obtained by making the frozen-core approximation and using the local spin density approximation. By repeating calculations for Ni_n ($n \leq 6$, $n = 13$) by including all electrons and by using the generalized gradient correction we demonstrated that these assumptions do not affect the calculated moment. (3) As indicated before, the magnetic moments are measured at the ambient cluster temperature, while the theory corresponds to 0 K. Since the energy levels near the HOMO are rather closely spaced, we expected that a structural change induced via rising temperature could affect the spin-up and -down levels, thus changing the moment. To assess this effect qualitatively, we used two random geometries accessed by Ni_7 and Ni_{13} at higher temperatures (101 and 401 K). The magnetic moments/atom computed for these geometries were the same as those computed for geometries at 0 K.

We now turn to a more critical examination of the experimental data. First as mentioned before, Apsel et al.[8] derived the intrinsic moments by assuming a superparamagnetic model. This model assumes that the anisotropy energy is small compared to thermal energy. The cluster then explores the entire distribution of orientations during its passage through the magnet and behaves like a paramagnetic atom. While this is a good first approximation, the shape, surface, and volume contributions to anisotropy can become significant at small sizes. For example, in the case of granular alloys of Fe in matrixes, Xia et al.[49] have measured a value of anisotropy energy per unit volume to be 2×10^7 erg/cm^3 for 20−40-Å particles. Using

the same value for clusters, one finds that Fe_n clusters having 120−140 atoms will have an anisotropy energy equivalent to a thermal energy at around 90 K. While there is no such measured data on nickel particles, one can expect a similar value for anisotropy energy. As shown by Jensen and Bennemann,[50] the inclusion of anisotropy contributions can have a quantitative effect on the moments derived using eq 7. Second, even if the superparamagnetic model were valid, one needs to know the precise temperature of the cluster to derive its magnetic moment (see eq 7). Determination of the cluster temperature has remained a controversial issue among experimentalists. Since there is no unambiguous method to derive the cluster temperature, the experimental magnetic moments obtained using eq 7 have to be regarded as tentative. In this context, we should point out that the magnetic moments measured by Apsel et al.[8] and de Heer and co-workers[7] are not in agreement. For example, de Heer et al. have observed that the moment of Ni_{200} is about $0.6\mu_B$; that is, it is almost bulklike. On the other hand, the moment of the Ni_{200} cluster measured by Apsel et al. is not bulklike and, indeed, disagrees with the experimental result of de Heer et al. by almost 50%. These authors did not study small Ni_n clusters. It will certainly be worthwhile for other authors to repeat the experiments on magnetic moments of Ni_n clusters for $2 \leq n \leq 1000$.

IV. Conclusions

This paper provides the first comprehensive study[51] of the electronic structure, vertical ionization potential, and magnetic moments of Ni_n clusters containing up to 21 atoms. The results were obtained from first principles using molecular orbital theory. The geometries of the clusters containing up to six atoms were globally optimized at the ab initio level, while those containing 7−21 atoms were obtained from a classical molecular dynamics simulation.

We have examined the effect of frozen-core and local spin density approximation by repeating the calculations for Ni_n ($n \leq 6$ and $n = 13$) that included all electrons and generalized gradient approximation. The geometries, bond distances, and magnetic moments were found to be insensitive to these approximations. While all-electron calculations had no effect on the binding energies and ionization potentials, the generalized gradient approximation lowered the magnitude of these values, bringing theory to much closer agreement with experiment.

The calculated ionization potentials at the local spin density approximation level of theory reproduce the experimental trend. However, to achieve quantitative agreement, inclusion of generalized gradient approximation in the exchange−correlation potential and temperature of the cluster will be needed.

The evolution of the electronic structure as clusters grow was probed by studying the molecular orbital energy levels. These approach a bandlike form for clusters as small as $n = 14$, implying that the electronic structure is bulklike. This in agreement with the photoemission studies of Wang and Wu. However, the calculated ionization potential for the $n = 21$ cluster is far from the bulk work function. Thus, different cluster properties evolve differently.

The magnetic moments of clusters were also calculated. Although these agree with the experimental trend qualitatively, serious quantitative discrepancies remain. Possible sources from both theory and experiment that could contribute to these discrepancies were critically examined. We came to the conclusion that the cluster temperature is at the heart of the problem, as the validity of the superparamagnetic model which was used to fit the experiment depends on the cluster temperature. We also argued that magnetism of clusters is not a simple surface phenomenon, as coordination number, interatomic distance, and specific symmetry influence the magnetic moment significantly. Thus, we showed that cluster magnetism cannot tell us anything about magnetism of crystal surfaces. Such studies in other transition metal systems such as Fe_n and Co_n will be very worthwhile.

Acknowledgment. This work is supported in part by a grant (DAAH04-95-1-0158) from the Army Research Office.

References and Notes

(1) *Small Particles and Inorganic Clusters*; Berry, R. S., Burdett, J., Castleman, A. W., Jr.; *Z. Phys.* **1993**, *26*. *Physics and Chemistry of Finite Systems: From Clusters to Crystals*; Jena, P., Khanna, S. N., Rao, B. K. Kluwer: Dordrecht, Netherlands, 1992. Bonacic-Koutecky, V.; Fantucci, P.; Koutecky, J. *Chem. Rev.* **1991**, *91*, 1035.

(2) Nayak, S. K.; Reddy, B.; Rao, B. K.; Khanna, S. N.; Jena, P. *Chem. Phys. Lett.* **1996**, *253*, 390; Nayak, S. K.; Rao, B. K.; Khanna, S. N.; Jena, P. *Chem. Phys. Lett.* **1996**, *259*, 588.

(3) Geusic, M. E.; Morse, M. D.; Smalley, R. E. *J. Chem. Phys.* **1985**, *82*, 590.

(4) Wang, L. S. Private communication. Wu, H.; Desai, S. R.; Wang, L. S. *Phys. Rev. Lett.* **1996**, *76*, 1441; Morse, M. D.; Hansen, G. P.; Langridge-Smith, P. R. R.; Zheng, L.-S.; Geusic, M. E.; Michalopoulos, D. L.; Smalley, R. E. *J. Chem. Phys.* **1984**, *80*, 5400.

(5) Lian, L.; Su, C.-X.; Armentrout, P. B. *J. Chem. Phys.* **1992**, *96*, 7542.

(6) Parks, E. K.; Zhu, L.; Ho, J.; Riley, S. J. *J. Chem. Phys.* **1994**, *100*, 7206; *J. Chem. Phys.* **1995**, *102*, 7377. Parks, E. K.; Riley, S. J. *Z. Phys. D* **1995**, *33*, 59.

(7) Billas, I. M. L.; Chatelain, A.; de Heer, W. A. *Science* **1994**, *265*, 1682.

(8) Apsel, S. E.; Emmert, J. W.; Deng, J.; Bloomfield, L. A. *Phys. Rev. Lett.* **1996**, *76*, 1441.

(9) Nayak, S. K.; Khanna, S. N.; Rao, B. K.; Jena, P. *J. Phys. Chem. A* **1997**, *101*, 1072.

(10) Blyholder, G. *Surf. Sci.* **1974**, *42*, 249.

(11) Adachi, H.; Tsukuda, M.; Satoko, C. *J. Phys. Soc. Jpn.* **1978**, *45*, 875.

(12) Basch, H.; Newton, M. D.; Moskowitz, J. W. *J. Chem. Phys.* **1980**, *73*, 4492.

(13) Rösch, N.; Ackerman, L.; Pacchioni, G. *Chem. Phys. Lett.* **1992**, *199*, 275. Rösch, N.; Knappe, P.; Sandl, P.; Görling, A.; Dunlap, B. I. In *The Challenge of d and f Electrons. Theory and Computations*; Salahub, D. R., Zerner, M. C., Eds.; ACS Symposium Series 394; American Chemical Society: Washington, DC, 1989; p 180.

(14) Nygren, M. A.; Siegbahn, P. E. M.; Wahlgren, U.; Akeby, H. *J. Phys. Chem.* **1992**, *96*, 3633.

(15) Wolf, A.; Schmidtke, H.-H. *Int. J. Quantum Chem.* **1980**, *18*, 1187.

(16) Tomonari, M.; Tatewaki, H.; Nakamura, T. *J. Chem. Phys.* **1986**, *85*, 2975.

(17) Pastor, G. M.; Dorantes-Davila, J.; Bennemann, K. H. *Chem. Phys. Lett.* **1988**, *148*, 459.

(18) Walch, S. P. *J. Chem. Phys.* **1987**, *86*, 5082.

(19) Fujima, N.; Yamaguchi, T. *J. Phys. Soc. Jpn.* **1989**, *58*, 3290.

(20) Gropen, O.; Almlöf, J. *Chem. Phys. Lett.* **1992**, *191*, 306.

(21) Andriotis, A. N.; Lathiotakis, N.; Menon, M. *Chem. Phys. Lett.* **1996**, *260*, 15.

(22) Estiú, G. L.; Zerner, M. C. *J. Phys. Chem.* **1994**, *98*, 9972.

(23) Panas, J.; Schüle, J.; Brandemark, U.; Siegbahn, P.; Wahlgren, U. *J. Phys. Chem.* **1988**, *92*, 3079 1988.

(24) Mlynarski, P.; Salahub, D. R. *J. Chem. Phys.* **1991**, *95*, 6050.

(25) Reuse, F. A.; Khanna, S. N. *Chem. Phys. Lett.* **1995**, *234*, 77.

(26) Stave, M. S.; Depristo, A. E. *J. Chem. Phys.* **1992**, *97*, 3386.

(27) Finnis, M. W.; Sinclair, J. E. *Philos. Mag.* **1984**, *50*, 45.

(28) Car, R.; Parrinello, M. *Phys. Rev. Lett.* **1985**, *55*, 2471.

(29) Sutton, A. P.; Chen, J. *Philos. Mag. Lett.* **1990**, *61*, 139.

(30) Kirkpatrick, S.; Gelatt, C. D., Jr.; Vecchi, M. P. *Science* **1983**, *220*, 671; Allen, M. P.; Tidesley, D. J. *Computer Simulation of Liquids*; Clarendon: Oxford, 1993. Briant, C. L.; Burton, J. J. *J. Chem. Phys.* **1975**, *63*, 2045.

(31) Hehre, W. J.; Radom, J. L.; Schleyer, P. V. R.; Pople, J. A. *Ab initio Molecular Orbital Theory*; Wiley: New York, 1986.

(32) Kohn, W.; Sham, L. J. *Phys. Rev.* **1965**, *140*, A1133.

(33) Hohenberg, P.; Kohn, W. *Phys. Rev.* **1964**, *136*, B864.

(34) Becke, A. D. *J. Chem. Phys.* **1988**, *88*, 2547. Lee, C.; Yang, W.; Parr, R. G. *Phys. Rev. B* **1988**, *37*, 786.

(35) *DMOL code*; Biosym Technologies, Inc.: San Diego.

(36) Frisch, M. J.; Trucks, G. W.; Schegel, H. B.; Gill, P. M. W.; Johnson, B. G.; Robb, M. A.; Cheeseman, J. R.; Keith, T.; Petersson, G. A.; Montgomery, J. A.; Raghavachari, K.; Al-Laham, M. A.; Zakrzewski, V. G.; Ortiz, J. V.; Foresman, J. B.; Closlowski, J.; Stefanov, B. B.; Nanayakkara, A.; Challacombe, M.; Peng, C. Y.; Ayala, P. Y.; Chen, W.; Wong, M. W.; Andres, J. L.; Replogle, E. S.; Gomperts, R.; Martin, R. L.; Fox, D. J.; Binkley, J. S.; Defrees, D. J.; Baker, J.; Stewart, J. P.; Head-Gordon, M.; Gonzalez, C.; Pople, J. A. *Gaussian 94*, Revision B.1; Gaussian, Inc.: Pittsburgh, PA, 1995.

(37) Knickelbein, M. B.; Yang, S.; Riley, S. J. *J. Chem. Phys.* **1990**, *93*, 94.

(38) Gantefor, G.; Eberhardt, W.; Weidele, H.; Kreisle, D.; Recknagel, E. *Phys. Rev. Lett.* **1996**, *77*, 4524.

(39) Wimmer, E.; Freeman, A. J.; Krakauer, H. *Phys. Rev. B* **1984**, *30*, 3113.

(40) Shintaku, K.; Mizutani, T.; Hosoito, N.; Shinjo, T. *J. Phys. Soc. Jpn.* **1991**, *60*, 1078. Korenivski, V.; Rao, K. V.; Birch, J.; Sundgren, J. E. *J. Magn. Magn. Mater.* **1995**, *140*−*144*, 549.

(41) Louderback, J. G.; Cox, A. J.; Lising, L. J.; Douglass, D. C.; Bloomfield, L. A. *Z. Phys. D* **1993**, *26*, 301.

(42) Reddy, B. V.; Khanna, S. N.; Dunlap, B. I. *Phys. Rev. Lett.* **1993**, *70*, 3323. Cox, A. J.; Louderback, J. G.; Bloomfield, L. A. *Phys. Rev. Lett.* **1993**, *71*, 923.

(43) Liu, F.; Press, M. R.; Khanna, S. N.; Jena, P. *Phys. Rev. B* **1989**, *39*, 6914.

(44) de Heer, W. A.; Milani, P.; Chatelein, A. *Phys. Rev. Lett.* **1990**, *65*, 488.

(45) Bucher, J. P.; Douglass, D. C.; Bloomfield, L. A. *Phys. Rev. Lett.* **1991**, *66*, 3052.

(46) Khanna, S. N.; Linderoth, S. *Phys. Rev. Lett.* **1991**, *67*, 742.

(47) Castro, M.; Jamorski, C.; Salahub, D. R. *Chem. Phys. Lett.* **1997**, *271*, 133.

(48) Dunlap, B. I. *Phys. Rev. A* **1990**, *41*, 5691.

(49) Xia, G.; Liou, S. H.; Taylor, J. N.; Chien, C. L. *Phys. Rev. B* **1986**, *34*, 7573.

(50) Jensen, P. J.; Bennemann, K. H. Private communication.

(51) Pacchioni, G. S.-C. Chung, Krüger, S.; Rösche, R. *Chem. Phys.* **1994**, *184*, 125. These authors had studied the evolution of cluster to bulk properties of Ni_n clusters $n = 6-147$ by confining the structure to either icosahedral or cuboctahedral shapes. As noted here and in ref 9, the real evolution of the structure of clusters does not follow any precise pattern and therefore is not indicative of real clusters.